

Giant Cell Tumor of the Thoracic Spine Simulating Mediastinal Neoplasm

Hideyuki Sakurai, Norio Mitsuhashi, Kazushige Hayakawa, and Hideo Niibe

Summary: A case of giant cell tumor of the thoracic spine simulating mediastinal neoplasm was identified on plain films, CT scans, MR images, and with scintigraphy. CT showed a hypervascular soft-tissue mass with shell-like calcification in the right upper mediastinum. MR imaging showed a collapse of the T1 vertebral body and a mass extending to the mediastinum. The mass had a low signal on T1-weighted MR images and a predominantly high signal on T2-weighted images with heterogeneity. Technetium-99m methylene diphosphonate bone scintigraphy showed intense uptake in both the T1 and marginal parts of the mediastinal mass. There was no accumulation of gallium-67 citrate, but 18-fluorine fluorodeoxyglucose positron emission tomography showed marked uptake. The variation in these imaging findings played an important role in the differential diagnosis of this uncommon mediastinal mass.

Giant cell tumor (GCT) of bone often arises from the long bones. Although the spine is the fourth leading location of GCT, the majority of these lesions occur in the sacrum (1). In several large series, only 1% to 2% of GCTs occurred in the thoracic spine (2–4). GCTs of the spine sometimes extend into the paraspinal soft tissue (1), but a primary thoracic spinal GCT simulating a huge mediastinal neoplasm is rare.

Case Report

A 34-year-old woman was admitted to the hospital with slight back pain and occasional difficulty swallowing. A posteroanterior projection chest film showed a well-defined oval mass in the right upper mediastinum (Fig 1A). CT showed an expansile soft-tissue mass associated with bone destruction of T1, involving both the vertebral body and right arch. The lesion had marginal shell-like calcification without a calcified matrix and showed signs of increasing density with contrast enhancement (Fig 1B–C). The tumor had a low signal on T1-

weighted MR images and a predominantly high signal on T2-weighted MR images, with mild heterogeneity (Fig 1D–E). Complete collapse of T1 was apparent on sagittal MR images of the thoracic spine (Fig 1F).

Various scintigraphic studies were performed for tissue characterization of this mediastinal mass. Both T1 and the marginal shell showed signs of increased uptake, but most of the tumor matrix had no accumulation revealed by technetium-99m methylene diphosphonate bone scintigraphy (Fig 1G). No accumulation was detected by gallium-67 citrate scintigraphy, but 18-fluorine fluorodeoxyglucose positron emission tomography showed remarkable uptake, with a standardized uptake value (5) of 5.8 (Fig 1H). The histologic specimen was diagnosed as a GCT of bone (Fig 1I).

Discussion

GCTs were termed “osteoclastomas” in the older literature because they were considered to arise from the osteoclast. The exact cell of origin, however, is unclear. The histologic appearance of GCT is a uniform distribution of multinucleated giant cells against a background of round to spindle-shaped mononuclear stroma cells, as shown in Figure 1I. Multinucleated giant cells can arise in bone in some conditions, including chondroblastoma, fibrous dysplasia, eosinophilic granuloma, chondromyxoid fibroma, telangiectatic or fibrogenic variants of osteosarcoma, and malignant fibrous histiocytoma (6).

In cases of spinal GCTs, there is usually an expansile lesion with bone destruction that affects the vertebral body, as opposed to the posterior elements observed with other spinal bone tumors, such as aneurysmal bone cyst, osteoid osteoma, and osteoblastoma (1). Because extension to the paraspinal soft tissue is often apparent, thoracic spinal GCT could simulate posterior mediastinal neoplasm. This report provides important information regarding diagnostic imaging in a case of GCT simulating a posterior mediastinal mass.

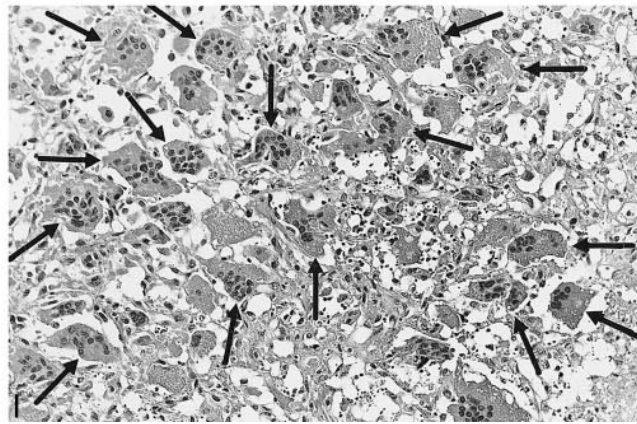
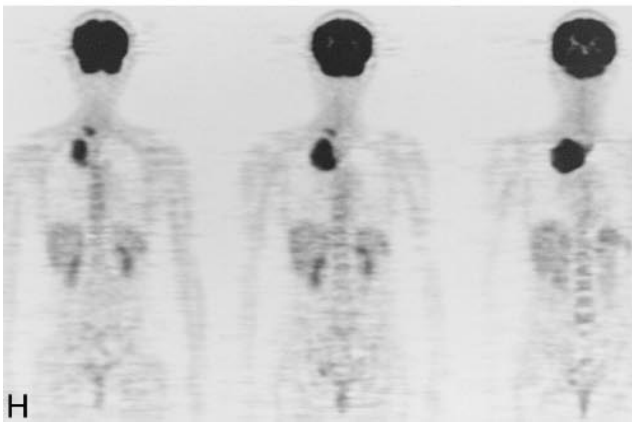
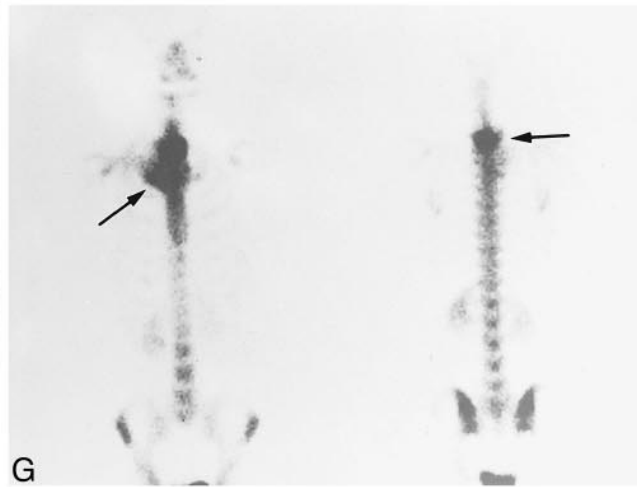
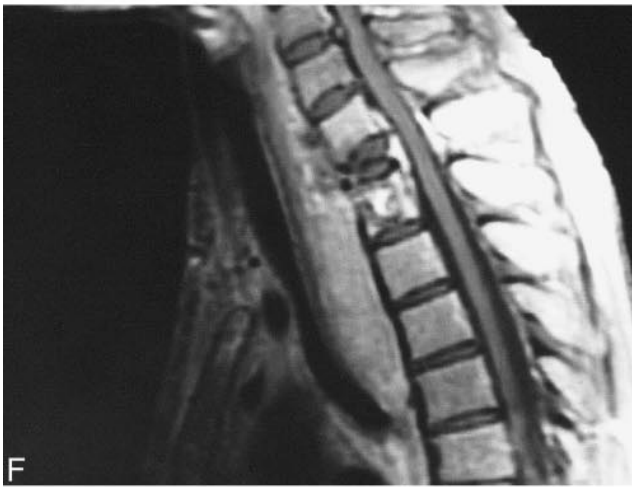
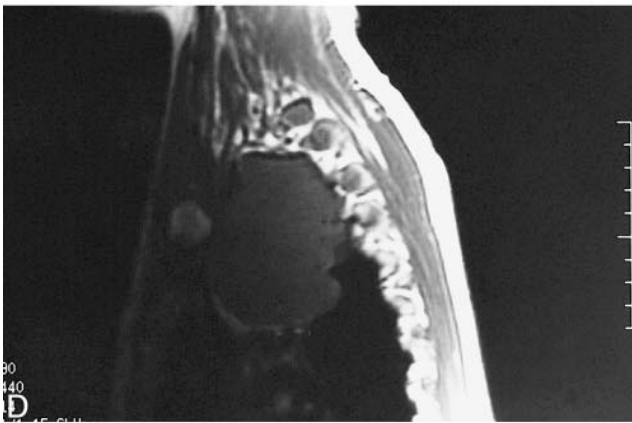
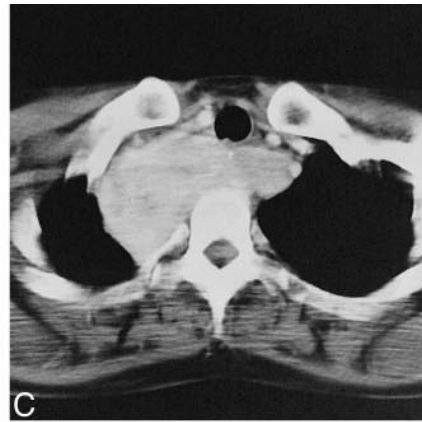
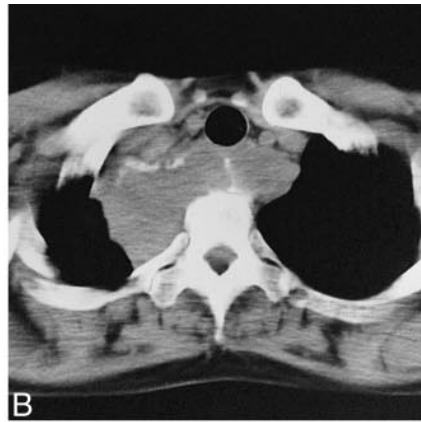
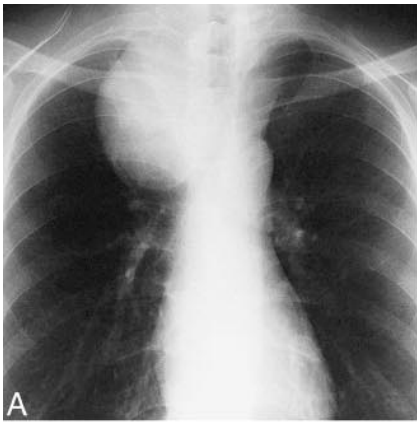
The radiographic characteristics of spinal GCT are considered to be a round or oval extrapleural mass with shell-like calcification of the marginal lesion and the absence of a mineralized matrix. One diagnostic possibility in spinal bone tumor is osteoblastoma, but an expansile lesion with multiple small calcifications is the most common appearance of spinal osteoblastomas (1). As a primary mediastinal tumor, one of the common posterior mediastinal neoplasms is a neurogenic tumor, but it may not destroy portions of the vertebral segment. On CT scans, a spinal GCT has been reported to show

Received April 19, 1999; accepted after revision June 1.

From the Department of Radiology and Radiation Oncology, Gunma University School of Medicine, 3-39-22 Showa-machi, Maebashi, Gunma 371-8511, Japan.

This work was supported in part by Grants-in-Aid from the Ministry of Education, Science and Culture of Japan (08770705, 09770673).

Address reprint requests to Hideyuki Sakurai, MD, Department of Radiology and Radiation Oncology, Gunma University School of Medicine, 3-39-22, Showa-machi, Maebashi, Gunma 371-8511, Japan.



a homogeneous hypervascular appearance with contrast enhancement (1). Heterogeneous density or a fluid level due to hemorrhage or necrosis within the GCT (1, 6) was not observed in our case.

The MR images provided more information on both tumor location and extension than did the CT images. For the differential diagnosis between primary vertebral tumor and primary mediastinal tumor, we diagnosed this tumor as a primary vertebral tumor because complete collapse of the T1 body was apparent on the MR images. If a large mediastinal tumor extended to the vertebral body, it might not only destroy the T1 vertebral body, but also destroy other surrounding vertebral bone. GCT usually has a low to intermediate signal on T1-weighted images and a predominantly high signal on T2-weighted images (7–9). It has been reported that a GCT shows several degrees of gadolinium enhancement on T1-weighted images (7, 10). On T2-weighted images, GCTs often have low to intermediate signal intensity caused by the relatively high collagen content of their fibrous components and the hemosiderin within the tumor (1, 11). Because most other spinal neoplasms have a high signal on T2-weighted images, the feature of hemosiderin deposition is reported to be useful for differential diagnosis.

GCTs have been noted to show increased peripheral activity on bone scintigraphy (the so-called doughnut sign) (12, 13). Because GCT commonly has peripheral calcification but has no calcification in the tumor matrix, the doughnut sign is considered to correlate with peripheral calcification of the tumor. In our case of technetium-99m methylene diphosphonate bone scintigraphy, uptake in T1 may correlate with vertebral bone destruction. Marked uptake in the marginal shell-like lesion in the anterior view may correlate with peripheral calcification of the tumor.

Few data exist regarding the tumor scintigraphy, such as in gallium-67 scintigraphic or positron emission tomographic studies. In our case, gallium-67 scintigraphy demonstrated no accumulation in the tumor. This supports the finding presented by Levine et al (13) that gallium-67 citrate scans ob-

tained in seven patients with GCTs of bone show slight uptake in four of seven cases and no uptake in three. They concluded that gallium-67 imaging was of limited use in the evaluation of suspected GCTs of bone. On the other hand, 18-fluorine fluorodeoxyglucose positron emission tomography showed remarkable uptake in our case. There has been no report in the literature of the use of 18-fluorine fluorodeoxyglucose positron emission tomography for GCT. The uptake of 18-fluorine fluorodeoxyglucose positron emission tomography has been considered to be an abundant activity of glucose metabolism. Recent studies indicated a relationship between glucose metabolism and cell proliferative activity, both in vivo and in vitro (14, 15). GCTs of bone, however, are basically slow-growing tumors compared with carcinomas, even if they show high histologic grade. We should consider that a remarkable 18-fluorine fluorodeoxyglucose positron emission tomographic accumulation in this case may indicate another mechanism of isotope uptake; for instance, high glucose metabolism of interstitial stromal cells in the tumor. These scintigraphic features may be overlapping with other mediastinal neoplasms, but they are important characteristics of scintigraphic findings in cases of spinal GCT.

Acknowledgments

We thank Dr. Jun Aoki, Department of Diagnostic Radiology, Gunma University Hospital, for valuable advice regarding the MR findings and Dr. Toshio Fukuda, Second Department of Pathology, Gunma University School of Medicine, for the pathologic diagnosis. In addition, we acknowledge the contributions of Drs. Yoshihiro Saito, Katsuya Maebayashi, and Sachiko Nasu, Department of Radiology and Radiation Oncology, Gunma University School of Medicine, who provided clinical assistance.

References

1. Murphey MD, Andrews CL, Flemming DJ, Temple HT, Smith WS, Smirniotopoulos JG. **From the archives of the AFIP. Primary tumors of the spine. Radiologic pathologic correlation.** *Radiographics* 1996;16:1131–1158
2. Schutte HE, Taconis WK. **Giant cell tumor in children and adolescents.** *Skeletal Radiol* 1993;22:173–176

←

FIG 1. Images from the case of a 34-year-old woman who was admitted to the hospital with slight back pain and occasional difficulty swallowing.

- A, Frontal chest roentgenogram shows a round mass in the right upper mediastinum.
- B, CT scan shows a well-defined soft-tissue density with marginal shell-like calcification. No calcification is seen within the mass.
- C, Contrast-enhanced CT scan shows that the mass enhances.
- D, T1-weighted MR image (repetition time, 440 milliseconds; echo time, 14 milliseconds) shows that the tumor has a homogeneous low signal.
- E, T2-weighted MR image (repetition time, 4000 milliseconds; echo time, 96 milliseconds) shows that the tumor has a predominantly high signal with some heterogeneity. The image also shows a peripheral low signal.
- F, Contrast-enhanced T1-weighted MR image (repetition time, 440 milliseconds; echo time, 14 milliseconds) shows homogeneous enhancement within the tumor. Complete collapse of the first thoracic spine and tumor spread to the second thoracic vertebral body are apparent. The extradural intraspinal mass effect can be seen.
- G, Bone scintigraph with technetium-99m methylene diphosphonate shows marked uptake both in T1 in the posterior view (*right arrow*) and in the marginal shell-like lesion in the anterior view (*left arrow*). Most of the tumor, however, shows no accumulation.
- H, Coronal view positron emission tomographic scan, with 18-fluorine fluorodeoxyglucose, shows uptake in the mediastinal tumor.
- I, Histologic specimen (hematoxylin and eosin stain; original magnification, $\times 400$) shows a uniform distribution of multinucleated giant cells (*arrows*) against a background of round to spindle-shaped mononuclear stroma cells.

3. Campanacci M, Baldini N, Boriani S, Sudanese A. **Giant-cell tumor of bone.** *J Bone Joint Surg Am* 1987;69:106-114
4. Dahlin DC. **Caldwell Lecture. Giant cell tumor of bone. Highlights of 407 cases.** *AJR Am J Roentgenol* 1985;144:955-960
5. Kim CK, Gupta NC, Chandramouli B, Alavi A. **Standardized uptake values of FDG. Body surface area correction is preferable to body weight correction.** *J Nucl Med* 1994;35:164-167
6. Lee MJ, Sallomi DF, Munk PL, et al. **Pictorial review. Giant cell tumours of bone.** *Clin Radiol* 1998;53:481-489
7. Meyers SP, Yaw K, Devaney K. **Giant cell tumor of the thoracic spine. MR appearance.** *AJNR Am J Neuroradiol* 1994;15:962-964
8. Tehranzadeh J, Murphy BJ, Mnaymneh W. **Giant cell tumor of the proximal tibia. MR and CT appearance.** *J Comput Assist Tomogr* 1989;13:282-286
9. Herman SD, Mesgarzadeh M, Bonakdarpour A, Dalinka MK. **The role of magnetic resonance imaging in giant cell tumor of bone.** *Skeletal Radiol* 1987;16:635-643
10. Yao L, Mirra JM, Seeger LL, Eckardt JJ. **Case report 715. Necrotic giant cell tumor of the femur.** *Skeletal Radiol* 1992;21:124-127
11. Aoki J, Tanikawa H, Ishii K, et al. **MR findings indicative of hemosiderin in giant-cell tumor of bone: frequency, cause, and diagnostic significance.** *AJR Am J Roentgenol* 1996;166:145-148
12. Veluvolu P, Collier BD, Isitman AT, Carrera GF, Hellman RS, Fry S. **Scintigraphic skeletal "doughnut" sign due to giant cell tumor of the fibula.** *Clin Nucl Med* 1984;9:631-634
13. Levine E, De-Smet AA, Neff JR, Martin NL. **Scintigraphic evaluation of giant cell tumor of bone.** *AJR Am J Roentgenol* 1984;143:343-348
14. Duhaylongsod FG, Lowe VJ, Patz E Jr., Vaughn AL, Coleman RE, Wolfe WG. **Lung tumor growth correlates with glucose metabolism measured by fluoride-18 fluorodeoxyglucose positron emission tomography.** *Ann Thorac Surg* 1995;60:1348-1352
15. Minn H, Clavo AC, Grenman R, Wahl RL. **In vitro comparison of cell proliferation kinetics and uptake of tritiated fluorodeoxyglucose and L-methionine in squamous-cell carcinoma of the head and neck.** *J Nucl Med* 1995;36:252-258